Image potential near a gradual interface between two dielectrics

Frank Stern
IBM Thomas J. Watson Research Center, Yorktown Heights, New York 10598
(Received 25 January 1978)

The image potential is calculated near a model interface in which the dielectric constant changes continuously in a thin transition layer between two dielectrics. If the transition is sufficiently smooth, the image potential is bounded and continuous, as opposed to the divergent and discontinuous $1/z$ dependence for an abrupt interface at $z = 0$. Results of model calculations of the image potential for the Si-SiO_2 and liquid-helium–vacuum interfaces are presented. Application of the model to the calculation of energy levels of electrons on liquid helium gives good agreement with the experimental results of Grimes *et al.* when an effective thickness of 0.57 nm is used for the helium-vacuum transition layer.

I. INTRODUCTION

The conventional[1] image potential for a charge Q near an interface between two dielectrics is

$$\phi_{\rm im}(z) = Q\delta/16\pi z\epsilon(z)\,, \tag{1}$$

$$\delta = (\epsilon_S - \epsilon_I)/(\epsilon_S + \epsilon_I)\,, \tag{2}$$

where ϵ_S is the permittivity (and $\kappa_S = \epsilon_S/\epsilon_0$ is the dielectric constant) of the dielectric occupying the half space $z > 0$, and ϵ_I and κ_I are the same quantities for the material occupying the half-space $z < 0$. The image potential energy is $V_{\rm im} = Q\phi_{\rm im}$, which is independent of the sign of Q. The image potential is attractive for charges on the low-dielectric-constant side of the interface and repulsive for charges on the high-dielectric-constant side of the interface.

This paper investigates the effect of a gradual transition between the two dielectrics, a subject which is of interest for several reasons. First, because the divergence and discontinuity of the image potential (1) are unphysical, a problem which has been addressed in the case of a jellium-vacuum interface.[2] Second, the image potential binds electrons near the surface of liquid helium[3,4] and affects the energy levels of electrons in space-charge layers near the Si-SiO_2 interface.[5-7] If some penetration of the electronic wave function across the interface occurs, the divergent image potential of Eq. (1) leads to problems. There is evidence, both for the Si-SiO_2 interface[7-9] and for liquid helium[10] that one or more atomic layers of intermediate bonding or density are present near the interface.

A model interface is examined in which the dielectric constant changes within a transition layer a few atomic diameters thick. We use a local dielectric function which depends only on the single space coordinate z, and is independent of the x and y coordinates. Such a model clearly ignores the atomic nature of the materials, and is therefore only an approximation to the behavior of real physical systems. In addition, our model ignores the mobile carriers which will modify the image potential at the interface between an insulator and a semiconductor.

We justify the present model in spite of these approximations by noting that it is consistent with the effective-mass-approximation approach that has been used to treat electrons near the Si-SiO_2 interface.[5-7] The gradual-transition-layer model has the advantage that its consequences, and their dependence on the values of physical parameters, can be easily tested.

II. THEORY

The electrostatic potential $\phi(\vec{\mathbf{r}})$ due to the presence of a point charge Q located at $\vec{\mathbf{r}}_0$ in a medium with a spatially varying permittivity ϵ is the solution of Poisson's equation

$$\nabla\cdot\epsilon\nabla\phi = -Q\delta(\vec{\mathbf{r}} - \vec{\mathbf{r}}_0)\,. \tag{3}$$

When ϵ is a function only of the z coordinate, we put the origin of the x and y axes at the position of the charge, introduce the two-dimensional radial coordinate R, and expand the potential in a Fourier-Bessel form:

$$\phi(\vec{\mathbf{r}}) = \int_0^\infty qJ_0(qR)A_q(z)\,dq\,, \tag{4}$$

where J_0 is the Bessel function of order zero. The coefficients $A_q(z)$ satisfy

$$A_q''(z) - q^2A_q(z) + [\epsilon'(z)/\epsilon(z)]A_q'(z) = -Q\delta(z - z_0)/2\pi\epsilon(z_0)\,, \tag{5}$$

where the primes indicate derivatives with respect to z. The boundary conditions are that $A_q(z) \to 0$ as $|z| \to \infty$. If the permittivity were independent of z, the solution of (5) would be

$$A_q^0(z) = [Q/4\pi\epsilon(z_0)q] \exp(-q\,|z - z_0|)\,, \tag{6}$$

and the potential would be the ordinary Coulomb potential $Q/4\pi\epsilon(z_0)\,|\vec{r} - \vec{r}_0\,|$, which diverges at the position of the point charge.

The image potential gives the effect of the spatially varying permittivity on the potential at the position of the point charge. It is given by

$$\phi_{\rm im}(z_0) = \frac{1}{2}\int_0^\infty B_q(z_0)\,dq\,, \tag{7}$$

$$B_q(z_0) = q[A_q(z_0) - A_q^0(z_0)]\,, \tag{8}$$

where the famous[11] factor $\frac{1}{2}$ arises because the image potential is a self-energy. The energy required to place a charge Q at the point $\vec{r}_0$ is the integral over Q from zero to its final value, which equals half of the value obtained by multiplying the charge by the potential obtained from the solution of Poisson's equation.

In Secs. III and IV we calculate the image potential for two different models of the interface.

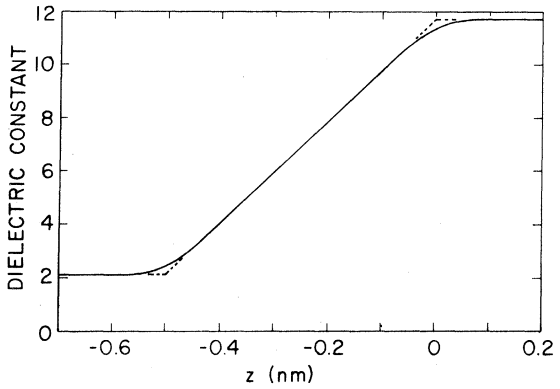

FIG. 1. Spatial variation of the dielectric constant $\kappa(z) = \epsilon(z)/\epsilon_0$ in the transition layer between two dielectrics for the two models used in this paper. The dashed line shows the linearly graded model of Sec. III and the solid line shows the smooth transition model of Sec. IV, with $a_t = 0.1$ nm. In both models $z_t = 0.5$ nm and the limiting values of the dielectric constant are taken to be $\kappa_I = 2.1$ and $\kappa_S = 11.7$.

III. LINEARLY GRADED TRANSITION

The simplest model for a transition layer is that the permittivity varies linearly:

$$\epsilon(z) = \epsilon_I + (\epsilon_S - \epsilon_I)S(z)\,, \tag{9}$$

where the grading function $S(z)$ for a layer of thickness z_s is given by

$$S(z) = \begin{cases} 0\,, & z < -z_t \\ (z + z_t)/z_t\,, & -z_t < z < 0 \\ 1\,, & 0 < z\,. \end{cases} \tag{10}$$

The resulting dielectric constant, with parameters $\kappa_S = 11.7$ and $\kappa_I = 2.1$ (the optical-dielectric constant) chosen for the Si-SiO_2 interface, is represented by the dashed line in Fig. 1. For this model, the solution for the amplitude coefficient $A_q(z)$ in the transition layer is

$$\begin{aligned} A_q(z) &= \alpha I_0(\eta) + \beta K_0(\eta)\,, \\ \eta &= q[z + \epsilon_S z_t/(\epsilon_S - \epsilon_I)]\,, \end{aligned} \tag{11}$$

where I_0 and K_0 are the Bessel functions of imaginary argument, and α and β are coefficients chosen to match boundary conditions. For large values of $|z|$ in the homogeneous dielectrics, we have $A_q(z) \sim \exp(-q\,|z|)$. We omit the straightforward but tedious details involved in matching boundary conditions in the solution of (5) and give only the results for the image potential amplitude $B_q(z_0)$ which enters in (7):

$$\begin{aligned} B_q(z_0) &= \frac{Q}{4\pi\epsilon_I}\,\frac{I_{1+}K_{3-} - K_{1-}I_{3+}}{I_{1-}K_{3-} - K_{1+}I_{3+}}\; e^{2q(z_0+z_t)}\,, \quad z_0 \le -z_t \\ &= \frac{Q}{4\pi\epsilon(z_0)}\left(\frac{4F_1F_3}{(I_{1-}K_{1-} - K_{1+}I_{3+})(I_{2-}K_{2-} - K_{2+}I_{2+})} - 1\right), \quad -z_t < z_0 < 0 \\ &= \frac{Q}{4\pi\epsilon_S}\,\frac{I_{1-}K_{3+} - K_{1+}I_{3-}}{I_{1-}K_{3-} - K_{1+}I_{3+}}\; e^{-2qz_0}\,, \quad 0 \le z_0 \end{aligned}$$

$$I_{j\pm} = I_0(\sigma_j) \pm I_1(\sigma_j)\,, \quad K_{j\pm} = K_0(\sigma_j) \pm K_1(\sigma_j)\,, \quad j = 1, 2, 3$$

$$F_1 = I_0(\sigma_2)K_{1+} - K_0(\sigma_2)I_{1-}\,, \quad F_3 = K_0(\sigma_2)I_{3+} - I_0(\sigma_2)K_{3-}\,,$$

$$\sigma_1 = qz_t\,\epsilon_I/(\epsilon_S - \epsilon_I)\,,$$

$$\sigma_3 = qz_t\,\epsilon_S/(\epsilon_S - \epsilon_I)\,,$$

$$\sigma_2 = \sigma_3 + qz_0\,. \tag{12}$$

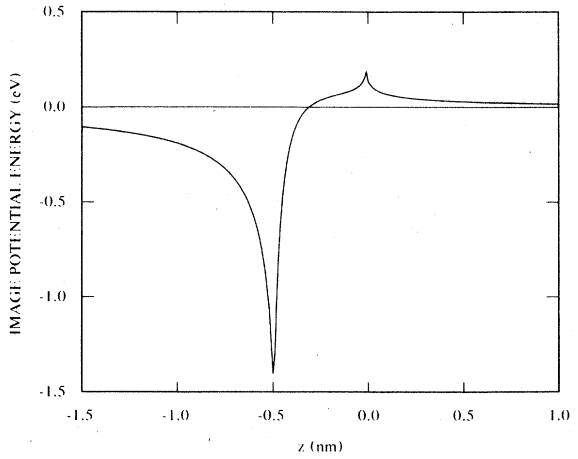

FIG. 2. Image potential for a model Si-SiO_2 interface with a linearly graded dielectric constant given by the dashed line in Fig. 1. The wave-vector dependence given in Eq. (13) has been used, with $q_c = 10^8$ cm^{-1}.

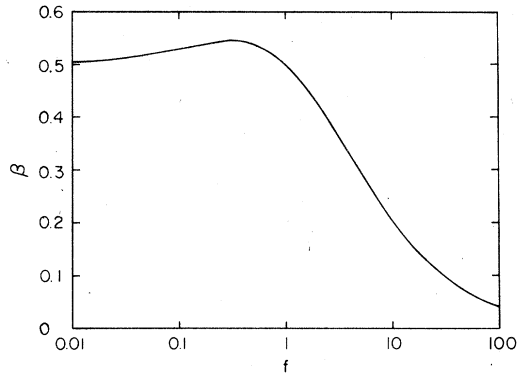

FIG. 3. Correction factor β of Eqs. (14)–(17), which enters in the asymptotic dependence of the image potential for a linearly graded transition layer, is plotted against $f = \epsilon_I/\epsilon_S$.

When z_0 is at either edge of the transition layer, $B_q(z_0) \sim 1/q$ for large values of q. This leads to a logarithmic divergence of the image potential at these two values of z_0. This divergence is integrable, in contrast to the $1/z$ divergence of the conventional image potential given in (1). But it is an unphysical singularity. One way to remove it is to round the corners of the grading function given in (10), as discussed in Sec. IV. Alternatively, we can introduce a q-dependent permittivity for which $\epsilon \to \epsilon_0$ for large values of q. The particular form we choose, suggested by the Penn model,[12] is

$$\epsilon_j(q) = \epsilon_0(q^2 + \kappa_j q_c^2)/(q^2 + q_c^2)\,. \tag{13}$$

where $j = I$ or S and where q_c is a convergence parameter.

Results for the image potential when q_c is taken to be 10^8 cm^{-1} are shown in Fig. 2 for the linearly graded Si-SiO_2 interface. Figure 2 shows that the image potential is indeed bounded and continuous, but the cusplike appearance near the edges of the transition layer shows that even the wave-vector convergence procedure introduced in (13) has not completely removed the effects of the sharp corner in the dielectric properties associated with the linear dependence assumed in this section. In Sec. IV we therefore consider a different model of the transition layer, in which the dielectric constant varies more smoothly and has a continuous first derivative.

The analytic solution obtained for the linearly graded model does allow an asymptotic expression to be obtained for the correction to the image potential associated with a transition layer of finite thickness. The expansion of $B_q(z_0)$ for small q gives, when $z_0 > 0$,

$$B_q(z_0) = (Q\delta/4\pi\epsilon_S)[1 - 2\beta(f)qz_t]e^{-2qz_0}\,, \tag{14}$$

$$\beta(f) = [\tfrac{1}{2} + f^2(1-f^2)^{-1}\ln f]/(1-f)\,, \tag{15}$$

where $f = \epsilon_I/\epsilon_S$. The function $\beta(f)$ is shown in Fig. 3. For large positive values of z_0 we find

$$\phi_{\rm im}(z_0) \sim (Q\delta/16\pi\epsilon_S)/[z_0 + \beta(f)z_t]\,. \tag{16}$$

Similarly, for large negative values of z

$$\phi_{\rm im}(z_0) \sim (Q\delta/16\pi\epsilon_I)/[z_0 + z_t - \beta(1/f)z_t]\,. \tag{17}$$

Equations (16) and (17) give the lowest-order correction to the image potential which results from the presence of the linearly graded transition layer of thickness z_t. They become unreliable when z_0 approaches the transition layer. For values of f close to unity, $\beta \simeq \frac{1}{2}$. The correction term then equals half the transition layer thickness, confirming the intuitive guess that at large distances the image potential is referred to the middle of the transition layer.

IV. SMOOTH TRANSITION

To avoid the singularities attributed to the discontinuous first derivative of the linearly graded permittivity used in Sec. III, we here consider a model in which this discontinuity is removed by introducing a sinusoidal rounding of the corners in the grading function $S(z)$ given in (10). We introduce an additional parameter a_t to characterize the amount of rounding, and write

$$S(z)=\begin{cases} 0, & z<-z_t-a_t \\ \{z+z_t+a_t-(2a_t/\pi)\cos[\pi(z+z_t)/2a_t]\}/2z_t, & -z_t-a_t<z<-z_t+a_t \\ (z+z_t)/z_t, & -z_t+a_t<z<-a_t \\ [z+2z_t-a_t+(2a_t/\pi)\cos(\pi z/2a_t)]/2z_t, & -a_t<z<a_t \\ 1, & a_t<z. \end{cases} \tag{18}$$

This model is illustrated by the solid curve in Fig. 1, where we use $z_t = 0.5$ nm and $a_t = 0.1$ nm. Note that a_t must lie in the range 0 to $\frac{1}{2}z_t$. The smoothed model of this section reduces to the model given in (10) when $a_t = 0$.

Poisson's equation, Eq. (5), has been solved numerically with the permittivity given by (9) and (18). As before, we require that $A_q(z) \sim \exp(-q|z|)$ for large $|z|$. These asymptotic dependences were factored out, and the differential equation which was solved numerically was the equation for the coefficient of the exponential. The equations were integrated inward from large values of $|z|$ and matched at $z = z_0$, where we require that $A_q(z_{0-}) = A_q(z_{0+})$ and

$$\left(\frac{dA_q}{dz}\right)_{z=z_{0+}} - \left(\frac{dA_q}{dz}\right)_{z=z_{0-}} = -Q/2\pi\epsilon(z_0). \tag{19}$$

The differential equation need only be solved within the transition layer, because outside the layer the relations

$$A_q(z_0)=\begin{cases} A_q(a_t)e^{2q(a_t-z_0)}, & a_t<z_0 \\ A_q(-z_t-a_t)e^{2q(z_0+z_t+a_t)}, & z_0<-z_t-a_t \end{cases} \tag{20}$$

obtain. $B_q(z_0)$ is calculated from the values of $A_q(z_0)$ using Eq. (8), and the image potential is calculated using Eq. (7). The integration over q in (7) must be carried to rather large values, especially near the edges of the transition layer. On the other hand, the numerical integration of the differential equation for A_q has been limited to values such that $qh_t \leq 0.3$, where h_t is the z-grid interval in the transition layer, because we used only centered first and second differences in solving Eq. (5). The contribution of large values of q to the integral in (7) was estimated by assuming that $B_q \sim q^{-2}$ for large q, a dependence which is suggested by our numerical results. The largest numerical errors occur in the region where the image potential is rapidly varying. They are estimated to be less than 3% of the maximum value of $|\phi_{im}(z_0)|$.

Figure 4 shows the calculated image potential found as described in this section, using the parameters from the full curve in Fig. 1 for a model Si-SiO_2 interface. Also shown is the image potential for a smaller value of the rounding parameter a_t.

Figure 5 shows the image potential for a smooth transition layer between liquid helium and its vapor.[3] The dielectric constants used are $\kappa_I = 1.057\ 23$ for liquid helium at 1 K,[13] and $\kappa_S = 1$. The transition layer has $z_t = 0.68$ nm and $a_t = 0.2$ nm; this choice of parameters is discussed in Sec. V. Note that the image potential in this case is much weaker than in the case of the Si-SiO_2 interface and that it is quite symmetric about the middle of the transition layer at $z = -0.34$ nm. Both results follow because of the small value of the parameter δ of Eq. (2), which is a measure of the dif-

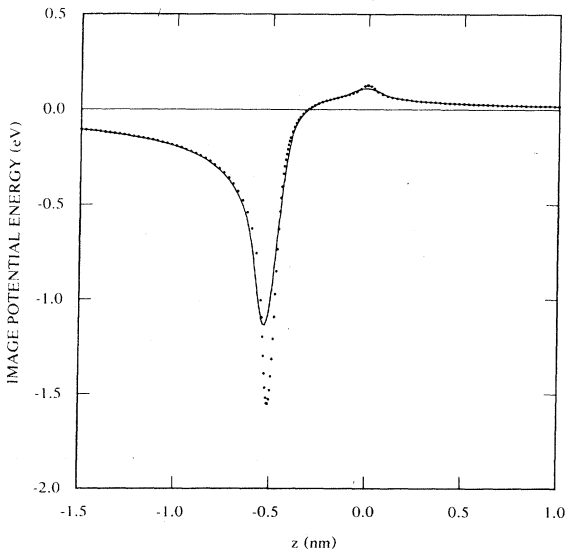

FIG. 4. Image potential for a model Si-SiO_2 interface with a smooth dielectric-constant transition. The solid curve is based on the dielectric constant given by the solid line in Fig. 1, with a rounding parameter $a_t = 0.1$ nm. The dotted curve is based on a transition layer with $a_t = 0.05$ nm.

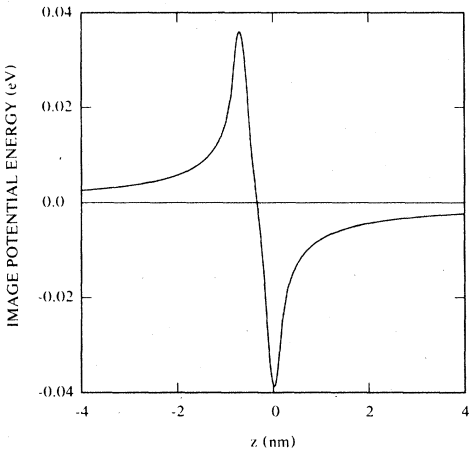

FIG. 5. Image potential for a model interface between liquid helium and its vapor, with a smoothly varying dielectric constant as in Sec. IV. The parameters used are $\kappa_I = 1.057\,23$, $\kappa_S = 1$, $z_t = 0.68$ nm, and $a_t = 0.2$ nm.

ference of the dielectric constants of the two media.

V. ENERGY LEVELS OF ELECTRONS ON LIQUID HELIUM

To test the model image potential described in Sec. IV, we use it to calculate the energy levels of electrons on the surface of liquid helium, for which precise experimental results are available.[4] The electronic states ψ_n, with energies E_n, are the solutions of

$$-\frac{\hbar^2}{2}\frac{d}{dz}\frac{1}{m^*}\frac{d\psi_n}{dz} + [V_b(z) - e\phi_{\rm im}(z) - e\phi(z) - E_n]\psi_n(z) = 0 , \quad (21)$$

where $\phi_{\rm im}(z)$ is the image potential described in Sec. IV, $V_b(z)$ is the barrier which tends to keep electrons out of the liquid helium, $\phi(z)$ is the electrostatic potential associated with an external electric field, if present, and m^* is the electron effective mass, which may be different from the free-electron mass when the electron is in liquid helium. The spatial dependence of V_b and m^* is assumed to follow the same grading function $S(z)$ that was used in Sec. IV for the dielectric constant. The barrier height varies from 1 eV in the liquid helium[3] to 0 in vacuum, and the effective mass varies from 1.1 m (Ref. 14) to m. The electrostatic potential is essentially given by $-eFz$, where F is the electric field in vacuum. The change of electric field on crossing into liquid helium has been taken into account, but has no significant effect on the results.

We look for bound-state solutions of (21), i.e., solutions for which $\psi(z) \to 0$ as $|z| \to \infty$. For a sharp interface, an infinite barrier height, and vanishing external electric field, the solutions form a hydrogenic spectrum:

$$E_n = -me^4\delta^2/512\pi^2\hbar^2\epsilon_0^2 n^2 , \quad (22)$$

where $\delta = (\kappa_{\rm He} - 1)/(\kappa_{\rm He} + 1)$. For $\kappa_{\rm He} = 1.057\,23$, we get $\delta = 0.027\,82$ and

$$\nu_n = E_n/h = -159.1/n^2 \text{ GHz} . \quad (23)$$

The energy separations found from the hydrogenic approximation are about 5% smaller than the values measured by Grimes *et al.*,[4] and there have been several attempts, using both phenomenological and microscopic models, to account for the discrepancy.[3,4,15,16]

In the present calculation we use the model already developed for the image potential near a gradual transition layer, treating the thickness parameter z_t as adjustable. The parameter a_t, which describes the rounding of the corners in the grading function S, has been fixed at 0.2 nm, partly on the basis of the shape of the transition layer found in previous work.[17-21]

Equation (21) has been solved for the levels $n = 1$, 2, and 3, and the energy separations $1 \to 2$ and $1 \to 3$ have been compared with the results of Grimes *et al.*[4] for no external field and in the limit of low-electron density. The best fit was obtained with $z_t = 0.68$ nm, which leads to an effective transition layer thickness [corresponding to the range $S(z) = 0.1$ to $S(z) = 0.9$] of 0.57 nm. This value is close to some of the previous estimates,[10,17,19] but there are both larger[20] and smaller[16,18] estimates.

Figure 6 gives the electric field dependence of the transition frequencies from $n = 1$ to $n = 2$ and 3. Our calculated results are compared with the experimental results of Grimes *et al.*[4] and with the variational results of their model calculation.

Some additional results for the solutions of Eq. (21) are given in Table I. For comparison with these results, note that the energies given in (23) for $F = 0$ are −159.1, −39.8, and −17.7 GHz for $n = 1$, 2, and 3, respectively, and that the expectation values of z for these three subbands are 11.4, 45.7, and 102.7 nm, respectively, in the hydrogenic approximation.

The good agreement between calculated and measured values of energy levels of electrons on liquid helium lends support to the validity of the smooth-transition model used here to describe the helium-vacuum interface, but by no means excludes other models. There are strong theoretical indications[19,21,22] that the density variation in the transition layer is neither symmetric nor monotonic. Tests of more detailed microscopic models of the interface should be carried out.

TABLE I. Calculated properties of electrons outside liquid helium in the presence of an electric field F in vacuum. ψ is the normalized wave function.

F (V/cm)		0			100	
n	1	2	3	1	2	3
E_n/h (GHz)	−166.2	−40.7	−17.9	−141.7	42.3	124.8
$\int_{-\infty}^{\infty} z\psi_n^2 dz$ (nm)	10.6	44.4	100.9	9.7	29.4	46.5
$\psi_n/(d\psi_n/dz)\|_{z=0}$ (nm)	0.42	0.42	0.42	0.42	0.42	0.42
$\int_{-\infty}^{0} \psi_n^2 dz$ (%)	0.0245	0.0029	0.0009	0.0279	0.0074	0.0049

VI. DISCUSSION

The main result of this paper is to show that a suitably smooth variation of the dielectric constant in a transition layer between two dielectrics leads to a smooth and bounded image potential through the interface. This result removes the bothersome singularity and discontinuity in the classical image potential given in Eq. (1). It then becomes easier to treat the behavior of electrons near such an interface—for example, electrons outside liquid helium, as described in Sec. V. Some calculations for electrons in a space-charge layer near a Si-SiO_2 interface have already been carried out[7] and indicate that there are significant changes in energy levels of subbands arising from different conduction-band valleys when a nonzero interface width and a finite barrier height are used. Additional calculations with more realistic assumptions for effective-mass variations and for the barrier heights seen by electrons in different valleys have been carried out, and will be prepared for publication later.

The values $z_t = 0.5$ nm and $a_t = 0.1$ nm which we have used for the Si-SiO_2 interface are estimates which have no definitive experimental or theoretical basis. Observation of the interface using x-ray photoelectron spectroscopy or Auger spectroscopy suggests a transition layer thickness ≥ 1 nm.[7-9] A model constructed by Pantelides and Long,[23] on the other hand, gives an atomically smooth interface. But even in that case there is at least one layer of atoms which will have Si atoms with bonding intermediate between that in Si and in SiO_2. Thus even a structurally smooth interface will yield a transition layer in the bonding and the effective potential which is at least two atomic layers thick, or about 0.3 nm in the Si-SiO_2 case. The transition layer for the dielectric constant is likely to be thicker than for the bonding. Analysis of internal photoemission results by DiStefano[24] indicates that there is little (≤ 0.05 eV) perturbation of the Si conduction-band edge for distances more than 0.4 nm from the nominal interface. That is not in disagreement with the parameters used in the present calculation, because the nominal interface is approximately in the middle of the transition layer.

Screening effects by mobile carriers will modify the image potential. In the Si-SiO_2 case, mobile carriers on the Si side of the interface will reduce the repulsive potential on that side and will increase the attractive potential on the insulator side of the interface. The image potential is a many-body effect which we have treated in a very crude

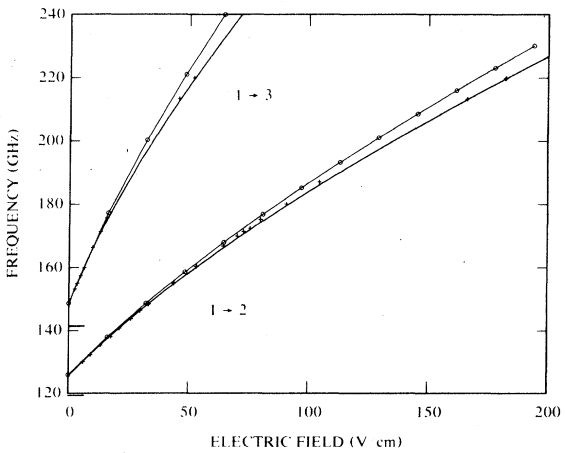

FIG. 6. Frequencies of transitions from the lowest subband ($n = 1$) to the first two excited subbands of electrons on liquid helium as functions of the externally applied electric field in vacuum. The points (+++) are the experimental results of Grimes *et al.*, Ref. 4, and the curves with open circles give the variational results of their model calculation. The solid curves are the results of the present calculation. The bars at zero field are the hydrogenic values from Eq. (23).

way here. The effects of mobile charges, of the atomic structure of the interface, and of the role of lattice polarization in forming the image should be studied in a more detailed investigation.

One general feature of the results in Figs. 2, 4, and 5 is the potential minimum on the low-dielectric-constant side of the transition layer. While the depth and shape of the minimum are model dependent, its existence should be common to all reasonable sets of parameters. Note that the image potential well is attractive for both positive and negative charges. This well, which binds electrons outside liquid helium, as discussed above, will not bind electrons in the Si-SiO_2 interface because it coincides with a large potential barrier that tends to keep electrons out of the oxide.[9] But the well could attract positive or negative ions, and may play a role in the tendency of charges to accumulate near the Si-SiO_2 interface.[25] A similar role for the image potential has been discussed in connection with metal-insulator interfaces.[26] But other effects, such as local bonding effects and interface strains, must also be considered.

Note added in proof. Recent experimental results[27] tend to confirm that the thickness of the Si-SiO_2 interface transition layer is close to the value assumed in the present calculation.

ACKNOWLEDGMENTS

I am indebted to C. J. Adkins, T. H. DiStefano, J. D. Dow, J. C. McGroddy, S. T. Pantelides, J. L. Pollmann, A. K. Rajagopal, and S. I. Raider for helpful comments and discussions, and to C. C. Grimes for supplying numerical values of the results in Fig. 2 of Ref. 4.

[1]See, for example, L. D. Landau and E. M. Lifshitz, *Electrodynamics of Continuous Media* (Pergamon, Oxford, 1960), p. 40.
[2]N. D. Lang and W. Kohn, Phys. Rev. B 7, 3541 (1973).
[3]M. W. Cole, Rev. Mod. Phys. 46, 451 (1974).
[4]C. C. Grimes, T. R. Brown, M. L. Burns, and C. L. Zipfel, Phys. Rev. B 13, 140 (1976).
[5]F. J. Ohkawa and Y. Uemura, Prog. Theor. Phys. Suppl. 57, 164 (1975).
[6]T. Ando, J. Phys. Soc. Jpn. 39, 411 (1975).
[7]F. Stern, Solid State Commun. 25, 163 (1977).
[8]S. I. Raider and R. Flitsch, J. Vac. Sci. Technol. 13, 58 (1976).
[9]R. Williams, J. Vac. Sci. Technol. 14, 1106 (1977).
[10]P. M. Echenique and J. B. Pendry, Phys. Rev. Lett. 37, 561 (1976).
[11]See, for example, J. Harris and R. O. Jones, J. Phys. C 7, 3751 (1974).
[12]D. R. Penn, Phys. Rev. 125, 2093 (1962).
[13]R. F. Harris-Lowe and K. A. Smee, Phys. Rev. A 2, 158 (1970).
[14]B. E. Springett, M. H. Cohen, and J. Jortner, Phys. Rev. 159, 183 (1967).
[15]H.-M. Huang, Y. M. Shih, and C.-W. Woo, J. Low Temp. Phys. 14, 413 (1974).
[16]T. M. Sanders, Jr., and G. Weinreich, Phys. Rev. B 13, 4810 (1976).
[17]C. C. Chang and M. Cohen, Phys. Rev. A 8, 1930 (1973).
[18]Y. M. Shih and C.-W. Woo, Phys. Rev. Lett. 30, 478 (1973).
[19]T. C. Padmore and M. W. Cole, Phys. Rev. A 9, 802 (1974).
[20]C. Ebner and W. F. Saam, Phys. Rev. B 12, 923 (1975).
[21]K. S. Liu, M. H. Kalos, and G. V. Chester, Phys. Rev. B 12, 1715 (1975).
[22]T. Regge, J. Low Temp. Phys. 9, 123 (1972).
[23]S. T. Pantelides, J. Vac. Sci. Technol. 14, 965 (1977).
[24]T. H. DiStefano, J. Vac. Sci. Technol. 13, 856 (1976).
[25]See, for example, C. T. Sah, IEEE Trans. Nucl. Sci. 23, 1563 (1976). I am indebted to Professor Sah for a preprint.
[26]C. G. Wang and T. H. DiStefano, Crit. Rev. Solid State Sci. 5, 327 (1975).
[27]*Proceedings of the International Topical Conference on the Physics of* SiO_2 *and its Interfaces*, edited by S. T. Pantelides (Pergamon, New York, to be published in 1978).